Hindawi
International Journal of Antennas and Propagation
Volume 2019, Article ID 8595104, 7 pages
https://doi.org/10.1155/2019/8595104

Research Article

Application of Compressive Sensing in Solving Monostatic Scattering Problems

Shui-Rong Chai,[1] **Li-Xin Guo**,[1] **and Long Li**[2]

[1]*School of Physics and Optoelectronic Engineering, Collaborative Innovation Center of Information Sensing and Understanding at Xidian University, Xi'an 710071, China*
[2]*School of Electronic Engineering, Xidian University, Xi'an 710071, China*

Correspondence should be addressed to Shui-Rong Chai; srchai1989@gmail.com

Received 5 June 2018; Accepted 11 November 2018; Published 17 January 2019

Academic Editor: Shiwen Yang

In this paper, a new CS-FMM method that conjugates compressive sensing (CS) with the fast multipole method (FMM) is proposed and validated to efficiently solve monostatic scattering from an arbitrary conducting target. The far zone scattered fields are viewed as the signal of interest. CS is introduced to reduce the number of computations. A new set of incident sources has been generated according to CS. By solving the matrix equations under the new set of incident sources and calculating the related far zone scattered fields, the measurements of the aforementioned signal can be derived. Then, the CS inversion is employed to reconstruct the desired monostatic far zone scattered fields by finding the smallest possible ℓ_1 norm solution. Monostatic radar cross section (RCS) from several conducting targets is studied by CS-FMM and by the traditional FMM. And the results are compared with each other to illustrate the accuracy and efficiency of the proposed method.

1. Introduction

Electromagnetic scattering from an arbitrary target has attracted a lot of attention over the past few decades for a large number of applications, such as target recognition and tracking, stealth target design, and radar surveillance. There exists many numerical methods that are proposed to analyze the electromagnetic scattering problems. For example, the method and moment (MoM) [1, 2], the shooting and bouncing ray (SBR) [3], and generalized method of moments [4, 5]. However, if monostatic scattering problem, which has wide incident angles, is interested, the aforementioned numerical methods need to obey the so-called Shannon-Nyquist sampling theorem to get a reasonable result. That is to say, the number of times to calculate the induced currents and the scattered fields is equal to the number of incident angles. This is time-consuming and typically leads to a huge amount of computational cost. Therefore, this is a very intuitive thinking that, in order to improve the efficiency of the aforementioned methods in solving the monostatic scattering problems while maintaining sufficient accuracy, one needs to reduce the sampling rate of the incident angles.

There exists a new sampling paradigm named compressive sensing (CS), which goes against the Shannon-Nyquist sampling theorem. The CS promises to measure the informative part of the signal directly at a rate significantly below the Nyquist rate and accurately reconstruct the signal from its lower dimensional measurements. Obviously, CS meets the requirement of reducing the number of calculations in monostatic scattering analysis. Therefore, several studies have been published in the literature to exploit the ideas from CS in solving the wide-angle electromagnetic scattering problems.

Carin et al. [6] are the first researchers that applied CS in solving wide incident angle scattering problems. He and his team of researchers at Duke University developed an in situ CS to reduce the number of computation required for target characterization by introducing the heterogeneous medium. D'Ambrosio [7] develops the ideas of Carin and integrates CS with the commercial software FEKO. Accordingly,

D'Ambrosio's method has both the benefits of CS and the deeply optimization benefits of FEKO. Chen et al. [8] and Chai and Guo [9, 10] attempt to combine the CS with the MoM for the purpose of efficiently analyzing two and three dimensional electromagnetic monostatic scattering problems. In [11], the triple hybrid approach that integrates the CS, the MoM, and the adaptive cross approximation (ACA) is proposed to further improve the efficiency of MoM in solving monostatic scattering problems. In [12] the hybrid method that conjugates CS with the multilevel fast multipole algorithm (MLFMA) is proposed, where the CS is utilized to reduce the number of incident angles. Wang et al. [13] propose a hybrid method that combines the CS with the characteristic basis function method (CBFM) for fast monostatic scattering analysis. The Bayesian compressive sensing together with the MoM is also utilized to solve monostatic scattering problems in [14].

In this paper, the hybrid method that conjugates CS with the FMM is proposed to efficiently analyze monostatic scattering problems. Different from the aforementioned methods, the new CS-FMM method proposed in this paper has its own advantages. First, the induced currents (or the Fourier transforms of the induced currents as in [6, 7]) on one patch over all incident angles are viewed as the proceeded signal, while the signal represents the monostatic scattered fields in the proposed CS-FMM. Second, there exists only one signal in our method, but the number of signals is n in the methods mentioned above, with n denotes the number of unknowns. Third, the new incident source is a linear combination of all plane waves in all of the aforementioned methods, while the new incident source in the newly proposed CS-FMM is a plane wave that derived by randomly extracting from the original incident waves. Fourth, the Gaussian random matrix is chosen to be the measurement matrix in all of the methods mentioned above except [12]. And the measurement matrix is the uniform sampling matrix in CS-FMM, which has a more concise form than that of the Gaussian random matrix. Fifth, the time expenditure on reconstructing the signal of CS-FMM is much smaller than that of the previous methods.

2. Theoretical Model

2.1. Traditional Fast Multipole Method. The results and discussion may be presented separately, or in one combined section, and may optionally be divided into headed subsections.

The purpose of solving a monostatic scattering problem is to evaluate the far zone monostatic scattered fields by

$$\mathbf{E}_{\text{sca}}(\theta) = -ik\eta \frac{\exp(ik\rho_0)}{4\pi\rho_0} \hat{k}_{\text{sca}} \times \hat{k}_{\text{sca}} \times \int_s \exp\left(-ik\boldsymbol{\rho}' \cdot \hat{k}_{\text{sca}}\right) \mathbf{J}\left(\boldsymbol{\rho}', \theta\right) ds', \tag{1}$$

where ρ_0 is the distance between the observation point and the original point, $\boldsymbol{\rho}'$ represents the position vector of the source point, $\hat{k}_{\text{sca}}$ is the unit vector of the scattered wave, θ denotes the incident and the scattering angle in the monostatic scattering analyzing, and $\mathbf{J}$ is the induced currents on the surface of the target, which can be described as

$$\mathbf{J}(\boldsymbol{\rho}, \theta) = \sum_{i=1}^{n} \alpha_i(\theta) \mathbf{f}_i(\boldsymbol{\rho}). \tag{2}$$

To compute $\mathbf{J}$ in (1) with traditional FMM, the following matrix equation can be derived:

$$\mathscr{A}\mathrm{T}\mathscr{D} I(\theta) = V(\theta), \tag{3}$$

where $\mathscr{A}$, T, and $\mathscr{D}$ denote the aggregation, transition, and disaggregation matrix, respectively. This three matrix can be constituted regardless of the choice of the incident angles, V is the known incident field vector, and I represents the unknown vector that formed by grouping the coefficients $\alpha_i(\theta)$.

By solving (3) under a particular incident angle θ_i, one can get the related unknown coefficients vector $I(\theta_i)$, and from $I(\theta_i)$ the induced current $\mathbf{J}(\boldsymbol{\rho}, \theta_i)$. Finally, the desired far zone scattered fields $\mathbf{E}_{\text{sca}}(\theta_i)$ can be computed by substituting the computed induced current $\mathbf{J}(\boldsymbol{\rho}, \theta_i)$ to (1).

It should be pointed out that the discussion in the previous paragraph is the calculating process of computing the scattered fields under one incident angle. Obviously one needs to repeat the previous process N time, if the monostatic scattering at hand has N incident angles. This is time-consuming and leads to a huge amount of computational cost. Therefore, CS is introduced to improve the efficiency of the FMM in solving monostatic scattering problems by reducing the number of times required to solve (3), (2), and (1).

2.2. CS-FMM. To introduce CS into the monostatic scattering problems, the far zone scattered fields are viewed as the signal of interest, which can be described as a complex column vector of length N in $\mathbb{C}^N$. It is clear that there exists just one such signal.

To facilitate the analysis, we rewrite (1) into the following matrix form:

$$\mathbf{E}_{N\times 1} = \text{diag}\,(\mathbf{G}_{N\times n} \mathbf{J}_{n\times N}), \tag{4}$$

where $\mathbf{E}$ and $\mathbf{J}$ denote the vector (or matrix) form of the far zone scattered fields and the induced currents, respectively. $\mathbf{G}$ is the matrix that generated by gathering the rest part on the right of (1). Definitely, $\mathbf{E}$ is the interested signal in CS-FMM.

CS attempts to integrate sensing and compression and therefore measure the informative part of the signal directly. Mathematically, the measurement process can be described by

$$\mathbf{s}_{m\times 1} = \Phi_{m\times N} \mathbf{E}_{N\times 1} = \Phi_{m\times N}\, \text{diag}\,(\mathbf{G}_{N\times n} \mathbf{J}_{n\times N}), \tag{5}$$

where Φ is an $m \times N$ matrix called the measurement matrix, m denotes the number of measurements, and $\mathbf{s}$ is the vector that represents the samples of the signal.

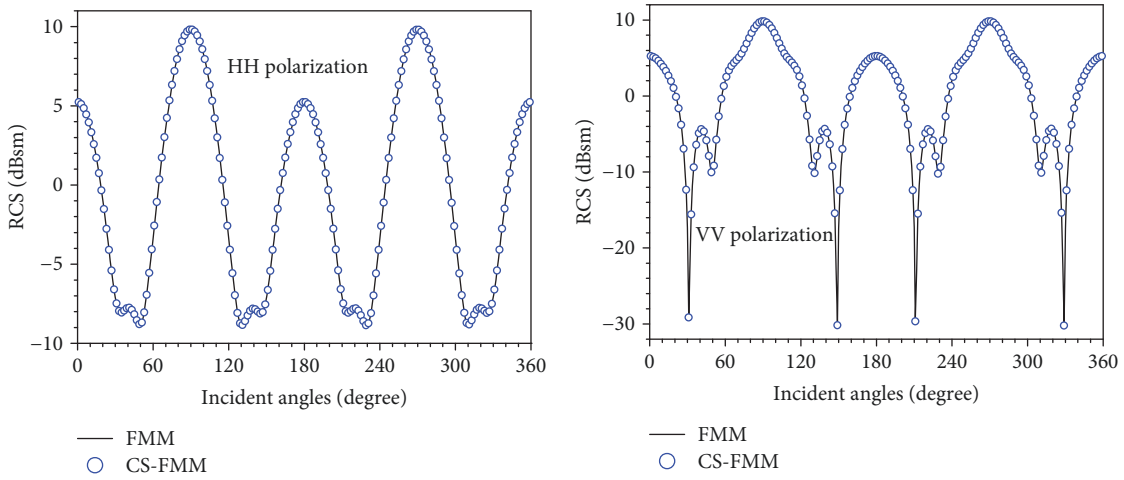

Figure 1: Monostatic RCS of the cylinder along *xoz* plane as functions of incident angles. (a) HH polarization; (b) VV polarization.

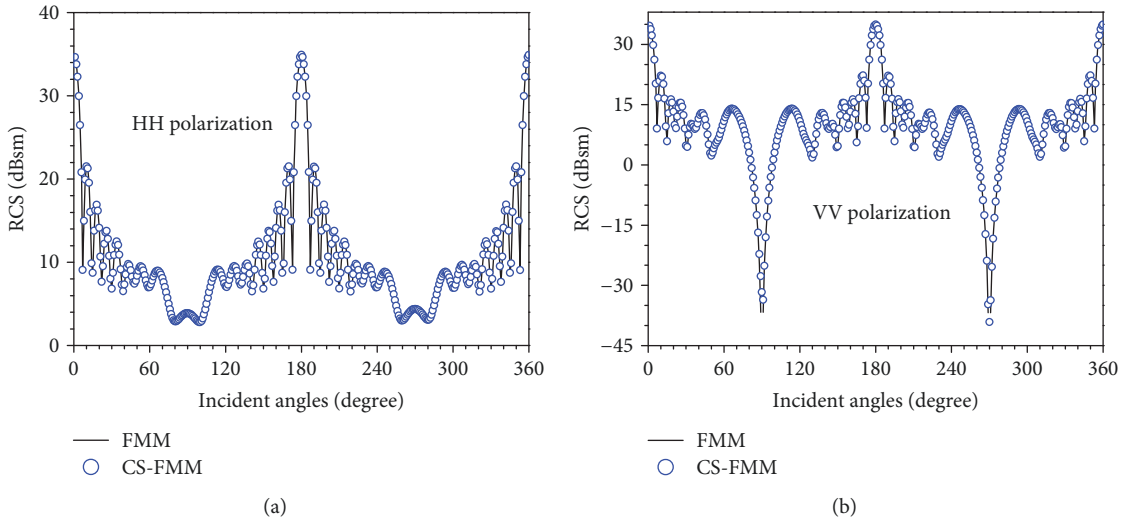

Figure 2: Monostatic RCS of the square plate along *xoz* plane as functions of incident angles. (a) HH polarization; (b) VV polarization.

The Gaussian matrix, which is a fully populated matrix, is arranged as the measurement matrix Φ in all of the previous works except [12], where the measurement matrix has a more concise expression. However, both the Gaussian matrix and the measurement matrix in [12] make the elements of $\mathbf{s}$ a linear combination of the elements of the signal $\mathbf{E}$. This makes it impossible to convert the measurement of the far zone scattered fields to the samples of the induced currents. Therefore, we introduce another type of measurement matrix named uniform sampling matrix, which is constructed as follows:

$$\Phi_{m\times N} = \begin{bmatrix} 0 & 1 & \cdots & 0 & 0 & 0 \\ 0 & 0 & \cdots & 1 & 0 & 0 \\ \vdots & \vdots & \ddots & \vdots & \vdots & \vdots \\ 1 & 0 & \cdots & 0 & 0 & 0 \end{bmatrix}, \quad (6)$$

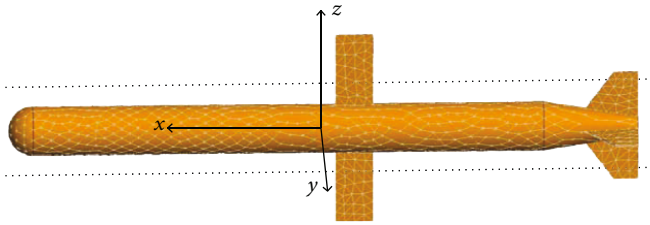

Figure 3: Missile model.

where each row has only one non-zero element that equals to one, and the position of the non-zero element is drawn from a discrete uniform distribution over 1 to N. Each row in the uniform sampling matrix can be interpreted as the selection of one incident angle, and there are totally m incident angles that are selected.

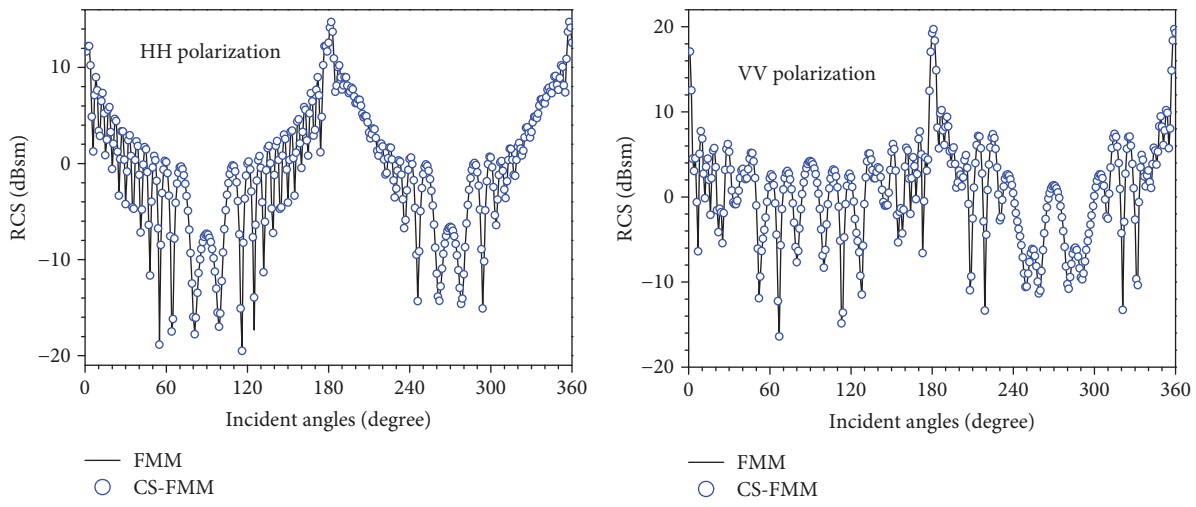

Figure 4: Monostatic RCS of the missile along *xoz* plane as functions of incident angles. (a) HH polarization; (b) VV polarization.

It can be found that, if the uniform sampling matrix is chosen as the measurement matrix, $\mathbf{s}$ can be generated by randomly constructing m elements of $\mathbf{E}$. And (5) can be rewritten as

$$\mathbf{s}_{m\times 1} = \tilde{\mathbf{E}}_{m\times 1} = \text{diag}\left(\tilde{\mathbf{G}}_{m\times n}\tilde{\mathbf{J}}_{n\times m}\right), \tag{7}$$

where $\tilde{\mathbf{G}}$ denotes the matrix that derived by randomly constituting m rows of $\mathbf{G}$. $\tilde{\mathbf{J}}$ represents the induced currents on the surface of the target under the selected m incident angles, which can be derived by solving the associated (3) m times.

Another point that should be emphasized is that the CS exploits the fact that the signal of interest is compressible itself or it is compressible in some sparse transform basis. In [15] we have examined that the electric field is compressible in FFT basis. Therefore, in the examples presented below, we choose fast Fourier transform (FFT) as the sparse transform basis.

Finally, the CS inversion is employed to recover the original far zone scattered fields by solving the following ℓ_1 norm optimization problem

$$\mathbf{E} = \Psi\hat{\mathbf{y}}; \quad \hat{\mathbf{y}} = \arg\min \left\|y'\right\|_1 \text{ s.t. } \Phi\Psi\hat{\mathbf{y}} = \mathbf{s}, \tag{8}$$

where Ψ is the sparse transform matrix, and $\mathbf{y}$ represents the corresponding coefficients vector. The orthogonal matching pursuit (OMP) [16] is applied to solve the ℓ_1 norm optimization problem described by (8) in this paper.

3. Numerical Results and Discussion

To demonstrate the accuracy and efficiency of the proposed CS-FMM, the radar cross section (RCS) from several conducting objects is evaluated. And the results are compared with those derived from traditional FMM. In performing the calculations some parameters are given as follows: the operating frequency is $f = 300$ MHz, the incident waves are assumed to be within the *xoz* plane, and the elevation angle

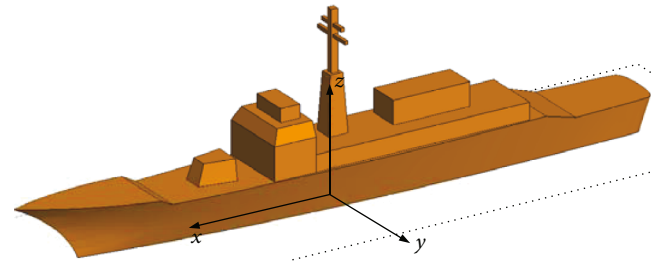

Figure 5: Ship model.

of the incident wave changes from 1° to 360°, with an interval of 1°. Accordingly, the traditional FMM has to solve (3), (2), and (1) 360 times to derive the wanted far zone scattered fields. The uniform sampling matrix and the FFT are chosen as the measurement matrix and sparse basis functions, respectively. All the simulations were performed on a computer with a 2.67 GHz processor (Intel Core i5 CPU) and 8.0 GB memory.

3.1. Cylinder. At first, the CS-FMM is applied to evaluate the monostatic RCS of a cylinder, which has a radius of 0.5 m and a length of 1.0 m. The cylinder axis is assumed to coincide with the x axis. During the simulation, the cylinder is dispersed into 1866 small triangles, which generate 2799 total unknowns, and the number of measurements is set as $m = 50$. In other words, the number of times required to solve (3), (2), and (1) is reduced to 50 by the introduction of CS theory. RCS distribution derived by CS-FMM and traditional FMM is depicted in Figure 1. It can be found that the two methods obtain almost the same RCS results.

3.2. Square Plate. To further verify the accuracy and efficiency of the proposed CS-FMM, the RCS of a square plate with an edge length of 4 m is computed by CS-FMM and by FMM. The tackled plate is located on the *xoy* plane and

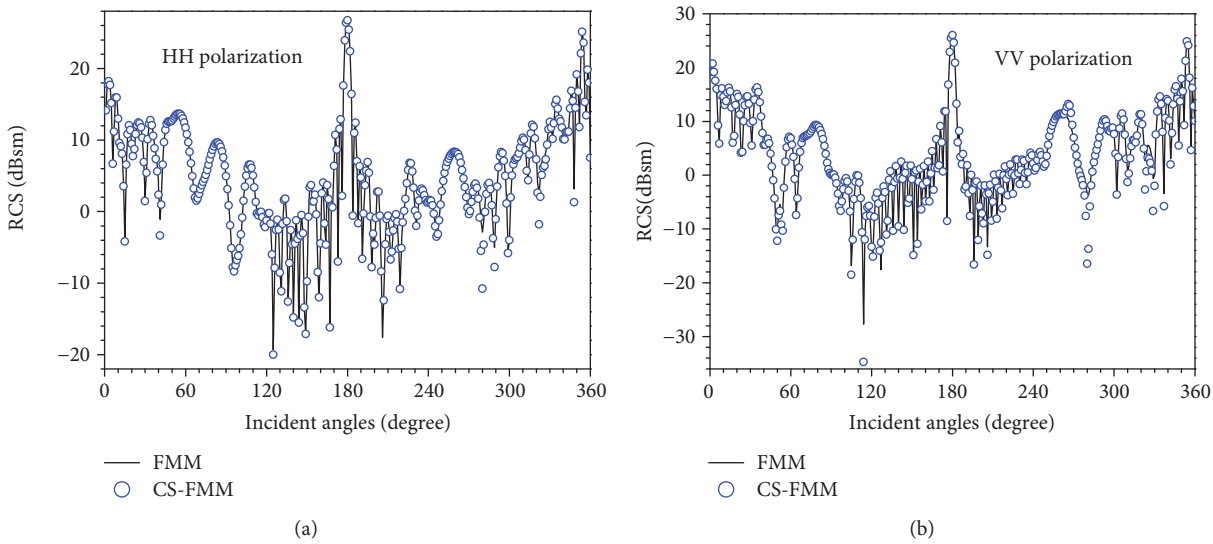

Figure 6: Monostatic RCS of the ship along *xoz* plane as functions of incident angles. (a) HH polarization; (b) VV polarization.

is partitioned into 2918 small triangles. The number of unknowns and measurements is 4305 and 95, respectively. RCS results of the FMM and CS-FMM along *xoz* plane are demonstrated in Figure 2. As shown in Figure 2, the CS-FMM yields approximately accurate results.

3.3. Missile. In this case, the proposed CS-FMM and the FMM are utilized to simulate the RCS distribution of a missile, which has a length of 6.7 m, width 0.52 m, and wingspan 3.18 m (as shown in Figure 3). Comparisons of RCS distribution derived from FMM and CS-FMM are shown in Figure 4. During the simulation, the missile is dispersed into 2748 small triangles, which generate 4122 total unknowns. In performing the simulation with CS-FMM, the number of measurements is chosen as $m = 180$. As can be observed in Figure 4, there is no visible difference between the two methods.

3.4. Ship. Finally, the angular distribution of the monostatic RCS from a ship (as shown in Figure 5) is simulated. The ship has a length of 9.8 m, width 1.2 m, and height 2.65 m. The number of unknowns in this case is 21129. And the number of measurements is set as $m = 180$ in CS-FMM. Monostatic RCS results are presented in Figure 6. It is easy to be observed that the two methods agree very well with each other.

The simulating time of the FMM and CS-FMM is summarized in Table 1. It is observed that the CS-FMM can save significantly over traditionally FMM method.

To provide a quantitative comparison of the number of measurements on the accuracy of the proposed method, the relative root mean square error (R-RMSE) of the far zone scattered fields is defined as follows:

$$\text{R-RMSE} = \frac{\|\mathbf{E}_{\text{CS-FMM}} - \mathbf{E}_{\text{FMM}}\|_2}{\|\mathbf{E}_{\text{FMM}}\|_2}, \quad (9)$$

where $\mathbf{E}_{\text{CS-FMM}}$ and $\mathbf{E}_{\text{FMM}}$ denote the far zone scattered fields derived by the proposed CS-FMM and the traditional FMM, respectively.

Table 1: Summary of simulating time of four models.

Model	Polarization	FMM (s)	CS-FMM (s)
Cylinder	HH	263	84
	VV	210	77
Square plate	HH	420	232
	VV	596	221
Missile	HH	747	437
	VV	606	393
Ship	HH	3087	1642
	VV	3728	2313

In the following, several functions (FFT, discrete cosine transform (DCT), Legendre polynomials, and the first order Chebyshev polynomials) are utilized as the sparse basis functions in the proposed CS-FMM. The detailed descriptions of the Legendre polynomials and the first order Chebyshev polynomials can be found in [17].

The justification for choosing FFT as the sparse basis functions in CS-FMM are presented in Figure 7. In Figure 7, the R-RMSE as a function of number of measurements (changed from 10 to 100) for different types of sparse basis functions is depicted. The aforementioned cylinder is chosen as the tackled target. Analogously, the uniform sampling matrix is set as the measurement matrix. Considering the random quality of the measurement matrix, for a given number of measurements, R-RMSE results for 1000 experiments are calculated and averaged. From Figure 7, one can find that the average R-RMSE obtained by FFT basis function is smaller than the other three types of basis functions for both HH and VV polarization. This means that the FFT provides a more accurate result than the other three types of basis functions for a given number of measurements. In another word, the FFT basis function can provide a sparsest representation of the signal. This is the reason why FFT is chosen as the basis function in the cylinder case simulation.

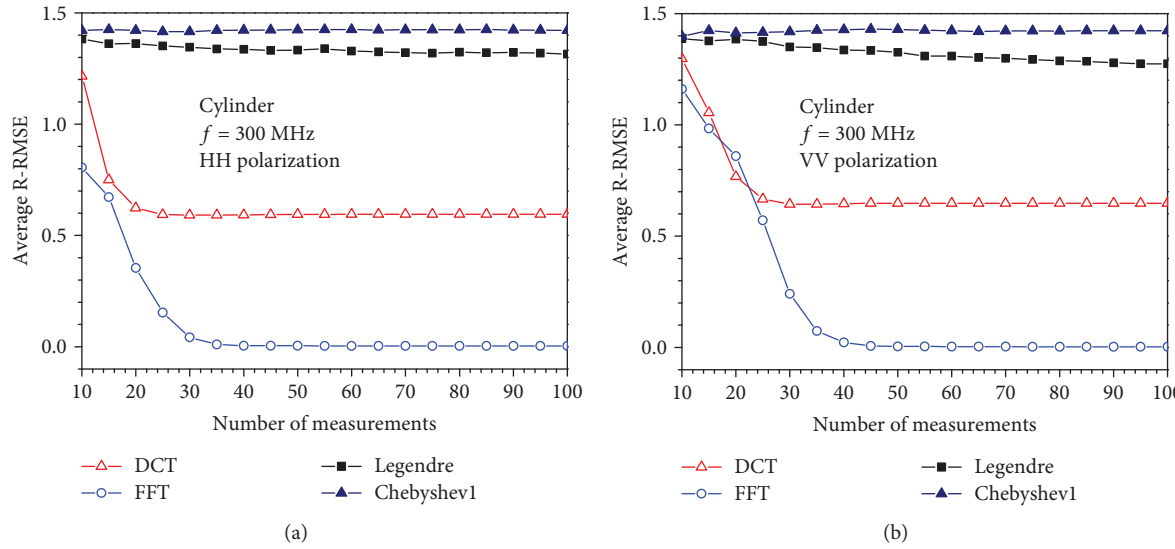

Figure 7: Average R-RMSE as a function of number of measurements for different types of sparse basis functions. (a) HH polarization; (b) VV polarization.

Meanwhile, $m = 50$ is chosen in the cylinder case to balance simulating time and accuracy. Analogously, similar results can be derived for plate, missile, and ship cases.

4. Conclusions

CS together with the FMM is introduced into monostatic scattering problems, and a new method named CS-FMM is proposed. The basic idea of CS-FMM is the sparse property of the far zone scattered fields. The CS is applied to exploit this sparsity and to reduce the number of computations. The FMM is worked as an electromagnetic solver. Numerical simulations show that the CS-FMM can improve the efficiency of traditional FMM dramatically in solving monostatic scattering problems.

Data Availability

All of the data used to support the findings of this study are included within the article.

Conflicts of Interest

The authors declare that they have no conflicts of interest.

Acknowledgments

This work was supported by the National Natural Science Foundation of China (Grant Nos. 41806210, 61871457, and 61431010), the China Postdoctoral Science Foundation (Grant Nos. 2018T111015, 2017M613067), the Fundamental Research Funds for the Central Universities (Grant No. JB170501), the 111 Project (Grant No. B17035), and the Foundation for Innovative Research Groups of the National Natural Science Foundation of China (Grant No. 61621005).

References

[1] W. C. Gibson, *The Method of Moments in Electromagnetics*, CRC Press, 2007.

[2] Y. Zhang and T. K. Sarkar, *Parallel Solution of Integral Equation-Based EM Problems in the Frequency Domain*, vol. 214, John Wiley & Sons, 2009.

[3] T.-Q. Fan and L.-X. Guo, "OpenGL-based hybrid GO/PO computation for RCS of electrically large complex objects," *IEEE Antennas and Wireless Propagation Letters*, vol. 13, pp. 666–669, 2014.

[4] D. L. Dault, N. V. Nair, J. Li, and B. Shanker, "The generalized method of moments for electromagnetic boundary integral equations," *IEEE Transactions on Antennas and Propagation*, vol. 62, no. 6, pp. 3174–3188, 2014.

[5] J. Li, D. Dault, N. Nair, and B. Shanker, "Analysis of scattering from complex dielectric objects using the generalized method of moments," *Journal of the Optical Society of America A*, vol. 31, no. 11, pp. 2346–2355, 2014.

[6] L. Carin, D. Liu, W. Lin, and B. Guo, "Compressive sensing for multi-static scattering analysis," *Journal of Computational Physics*, vol. 228, no. 9, pp. 3464–3477, 2009.

[7] K. D'Ambrosio, *Assessing the Benefits of Dct Compressive Sensing for Computational Electromagnetics*, Massachusetts Institute of Technology, Cambridge, MA, USA, 2010.

[8] M. S. Chen, F. L. Liu, H. M. Du, and X. L. Wu, "Compressive sensing for fast analysis of wide-angle monostatic scattering problems," *IEEE Antennas and Wireless Propagation Letters*, vol. 10, pp. 1243–1246, 2011.

[9] S. R. Chai and L. X. Guo, "Compressive sensing for monostatic scattering from 3D NURBS geometries," *IEEE Transactions on Antennas and Propagation*, vol. 64, no. 8, pp. 3545–3553, 2016.

[10] S. R. Chai and L. X. Guo, "A new method based on compressive sensing for monostatic scattering analysis," *Microwave and Optical Technology Letters*, vol. 57, no. 10, pp. 2457–2461, 2015.

[11] G.-h. Wang and Y.-f. Sun, "A hybrid approach for fast computation of multiple incident angles electromagnetic scattering

problems with compressive sensing and adaptive cross approximation," *International Journal of Antennas and Propagation*, vol. 2016, Article ID 1416094, 6 pages, 2016.

[12] H. Xin, H. Jun, and N. Zai-Ping, "Application of combination of excitations and compressed sensing for fast computation of monostatic scattering," in *2013 Cross Strait Quad-Regional Radio Science and Wireless Technology Conference (CSQRWC)*, pp. 136–139, Chengdu, China, 2013.

[13] Q.-Q. Wang, T. Jin, H.-B. Zhu, and R.-S. Chen, "Analyzing electromagnetic scattering using characteristic basis function method with compressed sensing," in *2013 6th International Congress on Image and Signal Processing (CISP)*, pp. 1633–1637, Hangzhou, China, 2013.

[14] H. H. Zhang, W. E. I. Sha, and L. J. Jiang, "Fast monostatic scattering analysis based on Bayesian compressive sensing," in *2017 International Applied Computational Electromagnetics Society Symposium - Italy (ACES)*, pp. 1-2, Firenze, Italy, 2017.

[15] S. R. Chai, L. X. Guo, K. Li, X. Meng, and L. Li, "Fast analysis of multi-static scattering problems with compressive sensing technique," *Journal of Quantitative Spectroscopy and Radiative Transfer*, vol. 202, pp. 136–146, 2017.

[16] J. A. Tropp and A. C. Gilbert, "Signal recovery from random measurements via orthogonal matching pursuit," *IEEE Transactions on Information Theory*, vol. 53, no. 12, pp. 4655–4666, 2007.

[17] H.-m. Du, M.-S. Chen, and X.-L. Wu, "The structure of the sparse basis function in compressive sensing for fast analysis of wide-angle monostatic scattering problems," in *2012 International Conference on Microwave and Millimeter Wave Technology (ICMMT)*, vol. 3, pp. 1–3, Shenzhen, China, 2012.